Quantitative 2-D Fuel Distribution Measurements in a Direct-Injection Gasoline Engine Using Laser-Induced Fluorescence Technique*

Taketoshi FUJIKAWA**, Yoshiaki HATTORI**,
Makoto KOIKE**, Kazuhiro AKIHAMA**,
Tatsuo KOBAYASHI*** and Souichi MATSUSHITA***

To improve the accuracy of fuel concentration measurements in a direct-injection gasoline engine by LIF (laser-induced fluorescence) technique, two approaches have been conducted. The combination of acetone as the fluorescence tracer of fuel and 266 nm as the excitation wavelength was used for the first approach in order to minimize the error caused by the temperature dependence of the LIF intensity. The second approach was the correction of the equivalence ratio obtained from the raw LIF image for the severe temperature distribution caused by evaporation and superheating of the injected fuel. The temperature distribution in the mixture was calculated; then the equivalence ratio was corrected for the effects of air density variation and the remaining LIF temperature dependence. This improved technique was applied to the quantitative analysis of the mixture formation process in a visualized direct-injection gasoline engine both under early and late injection conditions.

Key Words: Spectroscopic Measurement, Internal Combustion Engine, Fuel Injection, Laser Induced Fluorescence, Stratified Charge Combustion

1. Introduction

New types of spark-ignition (SI) engines which have a gasoline direct-injection (DI) system have been developed and have begun to be used in practice[1],[2]. The outstanding features of the engines are the great improvement in fuel economy as well as high output power compared with conventional port-fueled SI engines. These advantages are realized by a stratified combustion at partial loads and homogeneous combustion at higher loads. In this way, the mixture preparation and the combustion characteristics in the cylinder are significantly changed according to the engine operating conditions. Therefore, optimizing the in-cylinder mixture formation process is the key technology, because it dominates engine performance features such as fuel consumption, output power and exhaust emissions. Consequently, the development of a measurement technique which enables precise investigation of the mixture formation process is strongly required for the further development of DI gasoline engines.

The PLIF (Planar Laser-Induced Fluorescence) technique is a powerful tool for this purpose, because it allows instantaneous 2-D fuel distribution measurements[3]-[6]. In general, however, LIF intensity is affected not only by the fuel concentration but also by both the ambient temperature and pressure. This property of LIF causes a serious problem in the accuracy of the quantitative fuel concentration measurements in engines. The authors have reported the optimum combination of fluorescence tracer and excitation wavelength which features very low temperature and pressure effects on LIF intensity[7]. This technique facilitates the quantitative analysis of the mixture formation process in a port-fueled SI engine[8]. In the case of DI engines, the minimization of the temperature dependence of LIF intensity is still

* Received 2nd February, 1999
** Toyota Central Research & Development Laboratories, Inc., 41-1 Nagakute, Aich 480-1192, Japan. E-mail: fujikawa-t@mosk.tytlabs.co.jp
*** Toyota Motor Corporation, 1200 Mishuku, Susono 410-1193, Japan

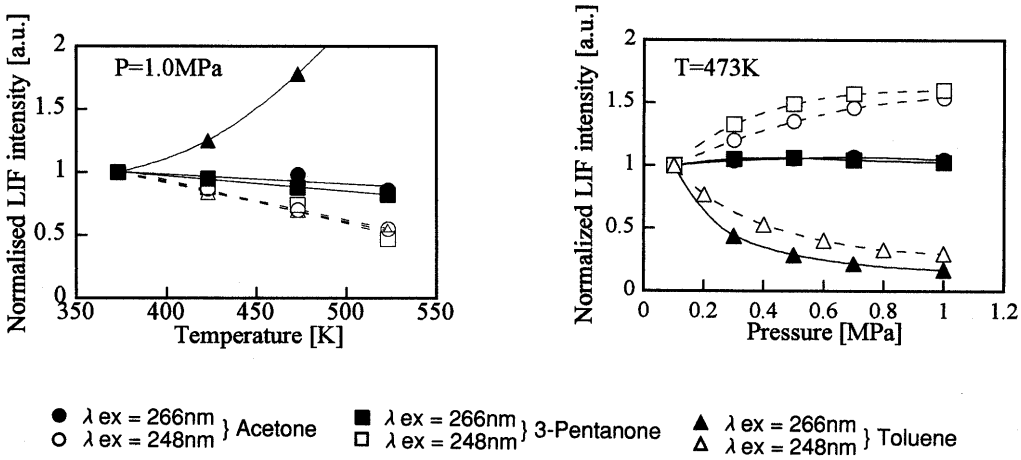

(a) Temperature effect on LIF intensity. LIF intensity is normalized by the value at 373K.

(b) Pressure effect on LIF intensity. LIF intensity is normalized by the value at 0.1 MPa.

Fig. 1 Temperature and pressure effects on LIF intensity for several combinations of fluorescence tracer and excitation wavelength taken using a constant volume vessel

important. However, even by the use of such a small temperature dependence combination, the temperature effect cannot be neglected because of the existence of severe temperature distribution in the mixture, which is caused by the evaporation and superheating of the fuel injected into the cylinder. Furthermore, when the fuel concentration is expressed in the form of the air/fuel ratio or the equivalence ratio, the results must be corrected for the increase in air density, which originates from the air temperature drop.

The objective of this study is to develop the method which can greatly improve the accuracy of fuel concentration measurements in a direct-injection gasoline engine by LIF technique. Firstly, the combination of fluorescence tracer and excitation wavelength we have reported[7],[8] was used in order to minimize the error caused by the temperature effect on LIF intensity. Secondly, the effects of the air density variation and remaining temperature dependence of LIF intensity were corrected for the equivalence ratio obtained from the LIF images. For the second purpose, temperature distribution caused by evaporation and superheating of the fuel injected into the cylinder was calculated. This improved technique was applied to the quantitative analysis of the mixture formation process in a visualized direct-injection gasoline engine both under early and late injection conditions.

2. Improvement in Measurement Accuracy

2.1 Fluorescence tracer and excitation wavelength

The selection of the fluorescence tracer and excitation wavelength is very important because it characterizes the temperature and pressure effects on LIF

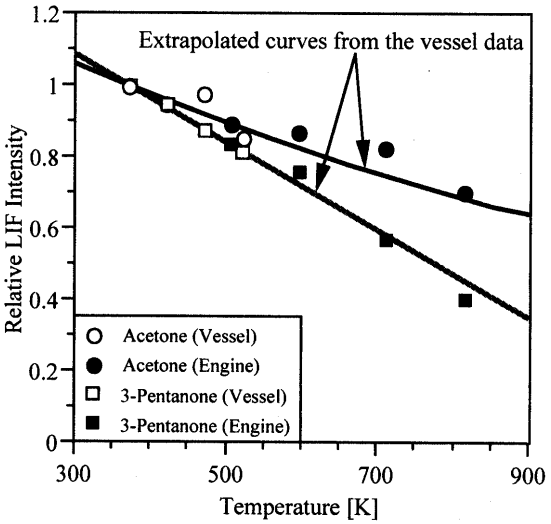

Fig. 2 Temperature dependence of LIF intensity of acetone and 3-pentanone excited at 266 nm taken using a constant volume vessel and a port-fueled SI engine

intensity. Figure 1 shows the temperature and pressure dependence on LIF intensity measured for some fluorescence tracers excited at 248 nm or 266 nm with a heated and pressurized constant volume vessel[7],[8]. It can be understood that the LIF intensity of acetone and 3-pentanone excited at 266 nm show lower temperature dependence compared with any other combinations. The pressure dependence of LIF intensity is also quite low with these combinations. On the other hand, even with these two tracers, the LIF intensity is strongly affected by the temperature and pressure variations when excited at 248 nm. Figure 2 shows the temperature dependence of the LIF intensities of acetone and 3-pentanone excited at 266 nm in the higher temperature region (500 - 800 K), which were

examined in our previous work conducted with a port-fueled SI engine[8]. Relative LIF intensity was derived from the LIF intensity and the tracer number density at the representative crank angle. The temperature is calculated from the in-cylinder pressure trace, which is described in section 2.5. The data obtained with the constant volume vessel and their extrapolated curves extended to the high temperature region are also indicated in the figure, which agree with the engine results fairly well. These results also prove the fact that the pressure dependence of LIF intensity is quite low. It can also be understood that 3-pentanone excited at 266 nm causes a more serious temperature effect on the LIF intensity than acetone; this tendency becomes more obvious in the high temperature region (>500 K). Based on these results, the quantitative fuel distribution measurements were made by the LIF of acetone excited at 266 nm. In this study, acetone was doped in iso-octane fuel at a concentration of 10% by weight.

A problem arises in that the boiling point of acetone (56.5°C) is lower than that of iso-octane (99°C). However, this effect may not cause a serious problem when the engine is fully warmed up and under the steady state condition, because of the following reasons.

(a) In the mixed solution, the evaporating temperature of each substance becomes closer than that of the solo substance[8].

(b) The piston surface temperature is higher than the boiling point of each substance.

(c) In the case of late injection, the in-cylinder gas temperature is assumed to be above 500 K, much higher than the boiling point of each substance.

2.2 Calculation of temporal equivalence ratio distribution

The temporal equivalence ratio distribution was calculated from LIF images taken with a visualized engine, as the first step. The raw LIF images were averaged over 16 consecutive cycles to reduce the effects of shot-noise of the intensified CCD camera, fluctuations of the laser sheet pattern and cycle-to-cycle variations in the engine. The temporal distribution of equivalence ratio $[\phi_{tp}]$ was then calculated based on the LIF image of the uniform mixture of predetermined equivalence ratio, ϕ_{uni}, using Eq. (1).

$$[\phi_{tp}]=C\cdot\phi_{uni}\cdot\frac{[\mathrm{LIF_{di}}]-[\mathrm{Back}]}{[\mathrm{LIF_{uni}}]-[\mathrm{Back}]} \qquad (1)$$

where

$[\phi_{tp}]$: temporal equivalence ratio distribution image,
$[\mathrm{LIF_{di}}]$: LIF image in DI operation,
$[\mathrm{LIF_{uni}}]$: LIF image in uniform mixture operation,
[Back]: background image without fuel injection,
ϕ_{uni}: equivalence ratio in uniform mixture operation,
C: correction factor for laser power fluctuation and window blur.

In Eq. (1), it is assumed that the equivalence ratio and the LIF intensity are in linear relation. With the combination of the acetone tracer and 266 nm excitation, this relation has been confirmed in our previous work using a port-fueled visualized engine[8], where the temperature distribution is not so severe. Equation (1) was applied to the images which were taken at the same crank angle for each engine operation. From this procedure, the pressure effect on the LIF intensity, which is essentially very low with this combination, is almost completely compensated because the in-cylinder pressure trace during the compression stroke shows no large difference between the DI and the uniform mixture operation.

2.3 Calculation of temperature distribution in mixture

As the second step, temperature distribution in the mixture, which is caused by the fuel injected into the cylinder, was calculated in order to make corrections for the temporal equivalence ratio. The procedure is basically the same as that which was carried out for the spray injected into a constant volume vessel[9] or a rapid compression machine[10], with the assumption that all the heat given to the fuel (the sensitive heat of the liquid fuel, the latent heat of vaporization and the heat for superheating the vapor) is supplied from the ambient gas and then both temperatures reach equilibrium temperature T_{eq}, namely;

$$m_f\left(\int_{T_{f0}}^{T_d} Cp_l dT + Hfg_{Td} + \int_{Td}^{T_{eq}} Cp_g dT\right) = -m_a\int_{T_a}^{T_{eq}} Cp_a dT \qquad (2)$$

where

m_f: mass of fuel (kg),
m_a: mass of ambient gas (kg),
T_{f0}: initial temperature of liquid fuel (K),
T_a: initial temperature of ambient gas (K),
T_d: boiling point of liquid fuel (K),
T_{eq}: equilibrium temperature of fuel and ambient gas (K),
Cp_l: specific heat of liquid fuel at constant pressure (kJ/kg·K),
Cp_g: specific heat of vapor fuel at constant pressure (kJ/kg·K),
Cp_a: specific heat of ambient gas at constant pressure (kJ/kg·K),
Hfg_{Td}: latent heat of fuel vaporization at T_d (kJ/kg).

From Eq. (2), the T_{eq} can be calculated for the air-fuel ratio (m_a/m_f), namely for the equivalence ratio ϕ, when T_a and T_{f0} are given. Figure 3 shows

the calculated results for the mixed fuel used in this experiment. Here, T_{f0} is assumed to be 323 K. For example, the temperature drop becomes about 160 K under the conditions of T_a=700 K and ϕ=3.0. This temperature drop changes the gas density as well as the LIF intensity. Consequently, the correction for this effect must be required to improve the measurement accuracy.

2.4 Correction for equivalence ratio

As the final step, the correction for the temperature is carried out for the temporal equivalence ratio. In practice, the initial value of ϕ is given by ϕ_{tp} and then the corrected value ϕ_c is calculated by the convergence method as shown in Fig. 4. Figure 5 shows the calculated results at T_a=700 K. For example, in the case of ϕ_{tp}=3.0, the corrected value ϕ_c becomes 2.2 at 266 nm excitation and 1.7 at 248 nm excitation, respectively. Figure 6 shows the correction rate for ϕ_c, which consists of the contributions of the air density change (A in Fig. 6) and temperature dependence of the LIF intensity (B in Fig. 6). In the case of 248 nm excitation, the total correction rate (A+B) itself is quite large and the major correction originates from the temperature dependence of LIF intensity (B_{248}). In the case of 266 nm excitation, on the other hand, the total correction rate becomes smaller and the major correction originates from the air density change (A), which value is the same as in the case of 248 nm excitation. Namely, in the case of 266 nm excitation, the correction for the temperature dependence of the LIF intensity (B_{266}) is very low. However, about 50% of the measurement error is estimated at ϕ_c=3.0 even in the case of 266 nm excitation, if there is no correction. This fact shows the importance of the correction described here.

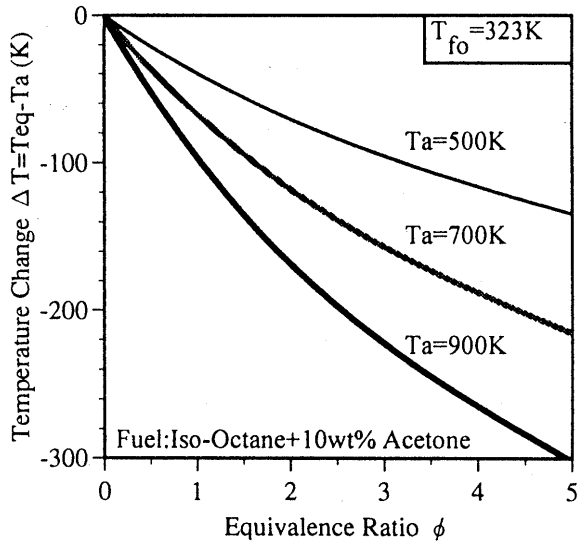

Fig. 3 Temperature change in ambient gas caused by fuel evaporation and superheating

2.5 Calculation of in-cylinder gas temperature in the engine experiments

The temporal equivalence ratio value for each pixel of the image [ϕ_{tp}] which was derived from Eq. (1) was corrected using the relation between ϕ_{tp} and ϕ_c as shown in Fig. 5. At this time, it became necessary to know the in-cylinder gas temperature T_a. It was calculated using the ideal gas equation from the in-cylinder pressure trace which was measured during the LIF imaging. The composition and the mass

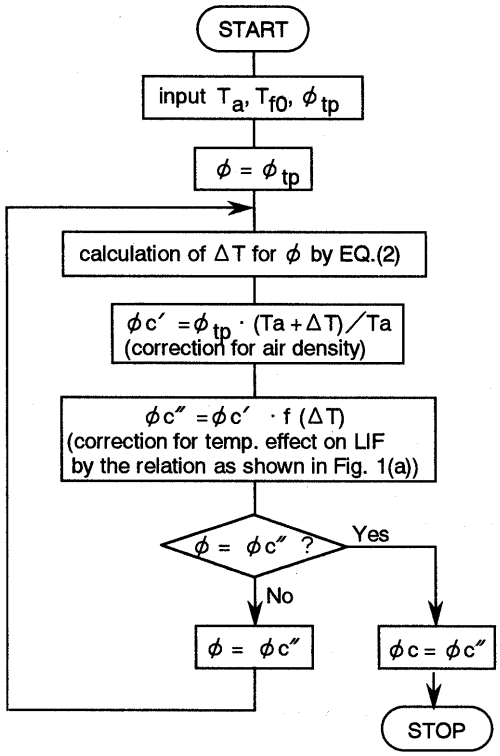

Fig. 4 Flow chart of correction for equivalence ratio

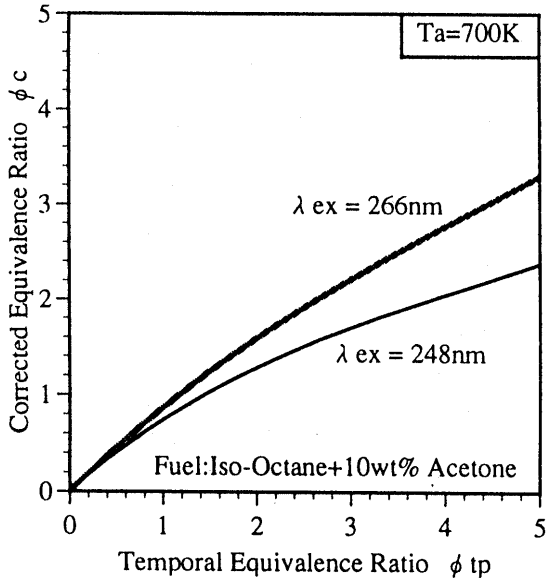

Fig. 5 Calculated results of equivalence ratio correction

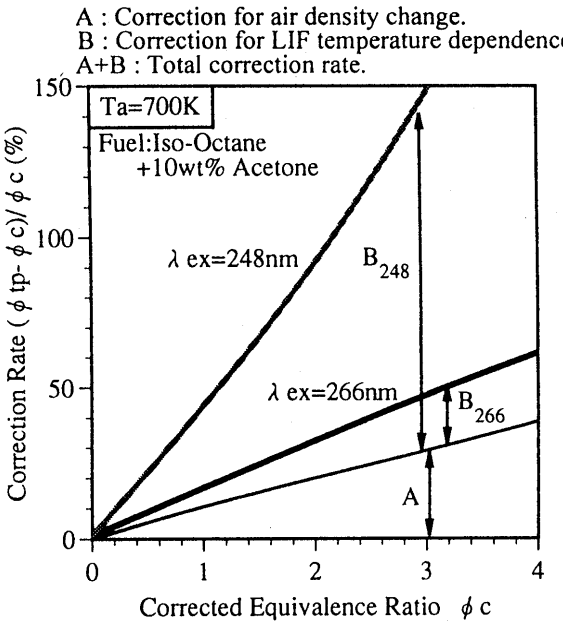

Fig. 6 Details of equivalence ratio correction

amounts of in-cylinder gases, which were required in the above calculation, were derived from the measured value of the charging efficiency, the injection amounts, and the residual gas ratio.

3. Application of the Correction Method to Engine Experiments

The technique described in the previous section was applied to the quantitative analysis of the mixture formation process in a direct-injection gasoline engine[1], using a visualized engine.

3.1 Experimental apparatus

3.1.1 Visualized engine A schematic of the visualized engine apparatus is shown in Fig. 7 The specifications of the engine are listed in Table 1. The engine is a 4-valve, pent-roof cylinder head, direct-injection, single cylinder, spark ignition engine. In-cylinder swirl flow is generated by the use of shrouded inlet valves. A swirl-type high pressure injector is mounted between two inlet ports. Fuel is injected into the narrow zone of the piston cavity. This zone is called the "mixture formation area". Another injector, which is an air-assist injector, is also used to make a pre-vaporized uniform mixture injected toward a porous electric heater which is placed in the inlet line 0.8 m upstream from the inlet ports.

The cylinder head has two quartz windows to permit the laser sheet passing through the combustion chamber. The inner surface of these windows is cylindrical in shape, while the shape of the outer surface has been specially designed to make light rays parallel both inside and outside of the cylinder head[11]. The engine performance test can be possible when these windows are replaced by metal dummies. An

Table 1 Specifications of the visualized engine

Number of cylinders	1
Displacement volume	500 cm^3
Bore	86 mm
Stroke	86 mm
Compression ratio	7.3
Number of valves	Inlet : 2 Exhaust : 2
Steady swirl ratio	2.4
Fuel Supply System	High Pressure Swirl Injector & Air-assist Injector
Fuel Pressure	12 MPa (Direct Injection) 0.3 MPa (Port Injection)

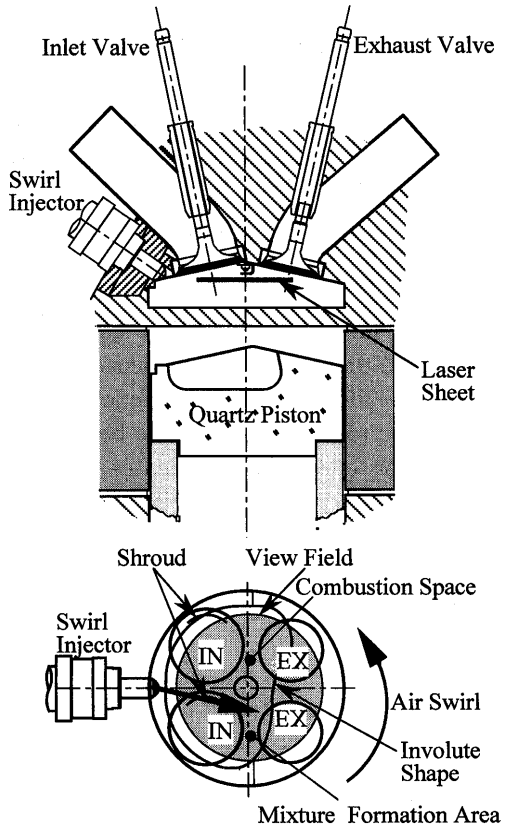

Fig. 7 Construction of the visualized engine

electromagnetic gas sampling valve can be attached to these dummy windows to measure the residual gas portion in the cylinder. A quartz piston is mounted at the top of elongated piston for observation from the piston bottom direction. This quartz piston has a unique involute-shaped cavity which is the same as that of a production engine.

3.1.2 Optical arrangement for LIF measurements A schematic of the LIF measurement apparatus for the visualized engine is shown in Fig. 8. The 4th harmonic of a Nd: YAG laser (Spectra Physics GCR-3) whose wavelength is 266 nm was used for the excitation light source. The mean laser power was 60 mJ/pulse. The laser light was split into two beams, both of which were formed into the horizontal laser

sheets and then introduced into the combustion chamber from the opposite side. Although the laser light is gradually absorbed by the tracer when it passes through the combustion chamber, the influence of laser intensity distribution caused by this absorption can be greatly reduced by this counter incidence method. In this experiment, such influence was below 1% under the severest condition. The location of each laser sheet (40 mm width×1 mm thickness) was at the plane of the ground electrode of the normal spark plug position; hence it had been moved 2 mm upward in the LIF measurements. A dual micro channel plate ICCD camera (Hamamatsu Photonics C4053) was used to detect the fluorescence images. An optical filter, transmitting above 350 nm in wavelength, was attached to the imaging lens (UV-Nikkor) to avoid the detection of the absorbed LIF light by acetone which has an absorption band below 340 nm. The shot-to-shot laser power fluctuation was monitored by utilizing a piece of the fluorescence block placed in the observation field as a reference image. A small part of the incident laser sheet was projected on the block, whose image was recorded with the fuel image simultaneously and used for the correction. The LIF images were recorded by a VTR and then analyzed by an image processing computer (Toshiba Tospix).

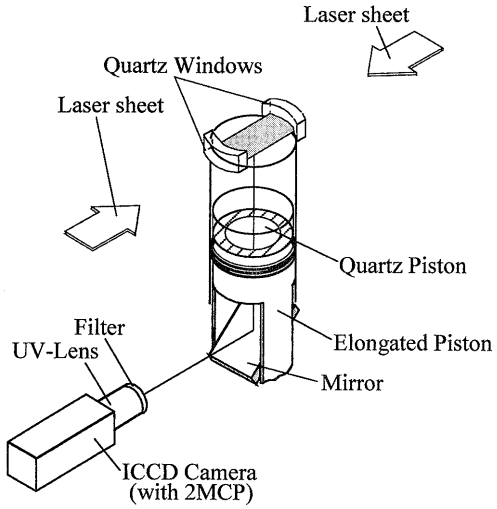

Fig. 8 Optical set-up for the LIF measurements

3.1.3 Experimental procedure The visualized engine was operated at a constant engine speed and charging efficiency. At the beginning of the experiment, the engine is operated under a port-fueled fired condition to heat the combustion chamber wall. After the exhaust emissions became almost stable, engine operation was switched to the uniform mixture combustion by an air-assist injector to take LIF images of the uniform mixture [LIF_{uni}] (in Eq. (1)) at the predetermined equivalence ratio ϕ_{uni} for each test crank angle. Next, the operating mode was changed to DI combustion and the DI LIF images [LIF_{di}] were taken. Finally, the background images [Back] were taken without fuel injection but with laser radiation. All LIF images were taken after the exhaust emissions became stable when the operating mode was changed. The engine operating conditions are listed in Table 2.

3.2 Results and discussion

The measured LIF images were processed according to the procedure explained in the previous section; then the corrected equivalence ratio distribution images were obtained.

3.2.1 Examination for correction Figure 9 shows the image processed results taken under the late (compression stroke) injection condition. The observation view field is the laser sheet portion inside the circle except for the blind region between the bottom and the sidewall of the cavity due to its small curvature. The lower part in Fig. 9 shows the

Table 2 Engine operating conditions

Engine speed	1200 rpm
Operation	Fired operation
Start of injection timing	-74° ATDC (late injection) -320° ATDC (early injection)
Overall equivalence ratio	0.65 (late injection) 0.85 (early injection)
Coolant Temperature	80 ℃

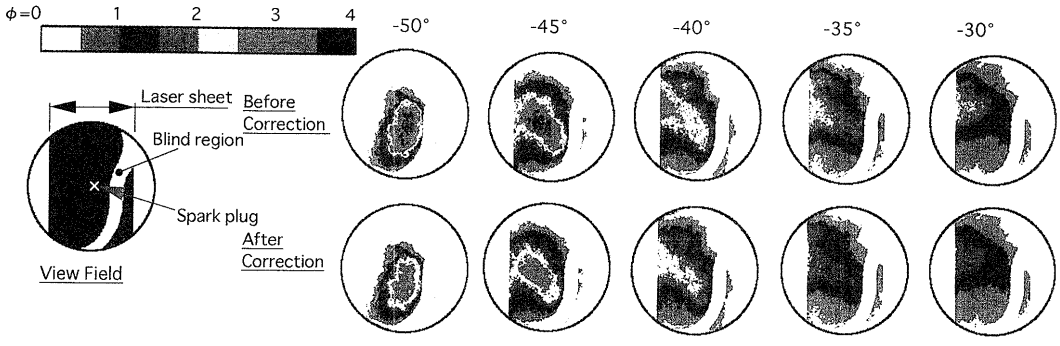

Fig. 9 Image-processed results of quantitative fuel distribution measurements in the late injection case, and the comparisons before and after correction

distribution of the corrected equivalence ratio, while the upper part shows the temporal images (before correction) derived from Eq. (1). The qualitative behavior of the mixture is not much different in either case. However, it is obvious that the value of the temporal equivalence ratio is expressed much higher than the corrected value even with the acetone and 266 nm excitation combination. Therefore, in the case of other combinations of fluorescence tracers and excitation wavelengths, more serious error is involved in the measurement results, if there is no correction.

In the following section, the mixture formation process is discussed based on the corrected equivalence ratio images.

3. 2. 2 Mixture formation under late injection

In Fig. 9, fuel is injected in the mixture formation area (see Fig. 7) so as not to wet the spark plug by fuel spray. Fuel evaporates in this area and then arrives at the laser sheet plane along the cavity surface around −50° ATDC. The equivalence ratio of the richest region in the mixture exceeds 2.5. After that, the mixture is diffused and moved toward the spark plug by air swirl motion (−50° to −30°). At the same time, the richest portion comes back slightly toward the injector due to the effect of the curved sidewall of the cavity. Spark plug fouling is further reduced because the richest mixture does not reach the spark position. Finally (−30°), the equivalence ratio around the spark plug becomes 1.0 - 1.5, suitable for ignition. The main portion of the mixture has moved to the combustion space in the cavity.

3. 2. 3 Mixture formation under early injection

Figure 10 shows the results taken under the early (intake stroke) injection condition. In this case, remarkable fuel stratification cannot be observed even at - 90°. An almost homogeneous mixture whose equivalence ratio is close to the overall equivalence ratio (ϕ=0.85) has been prepared prior to the end of the compression stroke (−30°).

From these measurements, the mixture formation concepts of this DI gasoline engine have been confirmed, quantitatively.

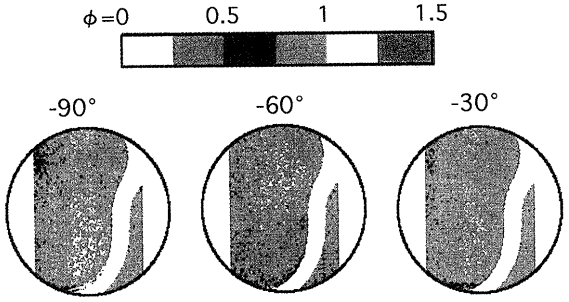

Fig. 10 Image processed results of quantitative fuel distribution measurements in the early injection case

4. Conclusions

(1) A method which improves the accuracy of quantitative fuel concentration measurements in a direct-injection gasoline engine by the LIF (laser-induced fluorescence) technique was developed. The combination of acetone as the fluorescence tracer of the fuel and 266 nm as the excitation wavelength was used in order to minimize the error caused by the temperature dependence of the LIF intensity. The correction of the equivalence ratio obtained from the raw LIF image was then carried out for the severe temperature distribution caused by evaporation and superheating of injected fuel. From these examinations, it was revealed that a considerable error is involved in the equivalence ratio which is directly calculated from the LIF intensity, even with the combination of acetone and 266 nm excitation. More serious error is inevitable with the use of other combinations of fluorescence tracers and excitation wavelengths, if there is no correction.

(2) This technique was applied to the analysis of the mixture formation process in a DI gasoline engine. In the case of late (compression stroke) injection, fuel evaporates in the mixture formation area and forms a rich mixture (ϕ>2.5). The mixture is then moved toward the spark plug, changing its concentration to a suitable value for ignition (ϕ=1.0 - 1.5) around the spark plug at ignition timing. In contrast to this, remarkable fuel stratification cannot be observed even at −90° in the case of early (intake stroke) injection. An almost homogeneous mixture whose equivalence ratio is close to the overall value has been prepared prior to the end of the compression stroke.

Acknowledgements

The authors would like to express their thanks to Dr. Kiyomi Kawamura of Toyota Central R & D Labs., Inc., for his technical support in image processing.

References

(1) Harada, J., Tomita, T., Mizuno, H., Mashiki, Z. and Ito, Y., Development of Direct-Injection Gasoline Engine, SAE Paper 970540, (1997).

(2) Iwamoto, Y., Noma, K., Nakayama, O., Yamauchi, T. and Ando, H., Development of Gasoline Direct Injection Engine, SAE Paper 970541, (1997).

(3) Shimizu, R., Matumoto, S., Furuno, S., Murayama, M. and Kojima S., Measurement of Air-Fuel Mixture Distribution in a Gasoline Engine Using LIEF Technique, SAE Paper 922356, (1992).

(4) Berckmüller, M., Tait, N.P., Lockett R.D. and Greenhalgh, D.A., In-Cylinder Crank-Angle-

Resolved Imaging of Fuel Concentration in a Firing Spark-Ignition Engine Using Planar Laser-Induced Fluorescence, 25th Symposium (International) on Combustion, (1994), p. 151.

(5) Ghandhi, J.B. and Bracco, F.V., Mixture Preparation Effects on Ignition and Combustion in a Direct-Injection Spark-Ignition Engine, SAE Paper 962013, (1996).

(6) Urushihara, T., Kakuhou, A., Itoh, T. and Takagi, Y., LIF Visualization of In-cylinder Mixture Formation in a Direct Injection SI Engine, Proceeding of the 14th Internal Combustion Engine Symposium, Japan, (in Japanese), No. 9737752, (1997), p. 523.

(7) Akihama, K. and Fujikawa, T., Temperature and Pressure Dependence of LIF Intensity of Some Tracers for 2-D Fuel Distribution Measurement, Proceeding of 24th Symposium on Visualization (Japan), (in Japanese), Vol. 16, No. 1 (1996), p. 161.

(8) Fujikawa, T., Hattori, Y. and Akihama, K., Quantitative 2-D Fuel Distribution Measurements in an SI Engine Using Laser-Induced Fluorescence with Suitable Combination of Fluorescence Tracer and Excitation Wavelength, SAE Paper 972944, (1997).

(9) Senda, J., Kanda, T., Kobayashi, M. and Fujimoto, H., Quantitative Analysis of Fuel Vapor Concentration in Diesel Spray by Exciplex Fluorescence Method, SAE Paper 970796, (1997).

(10) Yen, C., Kamimoto, T., Kosaka, H. and Kobori, S., Quantitative Measurement of 2-D Fuel Vapor Concentration in a Transient Spray via a Laser-Induced Fluorescence Technique, SAE Paper 941953, (1994).

(11) Fujikawa, T., Ozasa, T. and Kozuka, K., Development of Transparent Cylinder Engines for Schlieren Observation, SAE Paper 881632, (1988).